Cecilia Heldmann
Lund University
June 2014

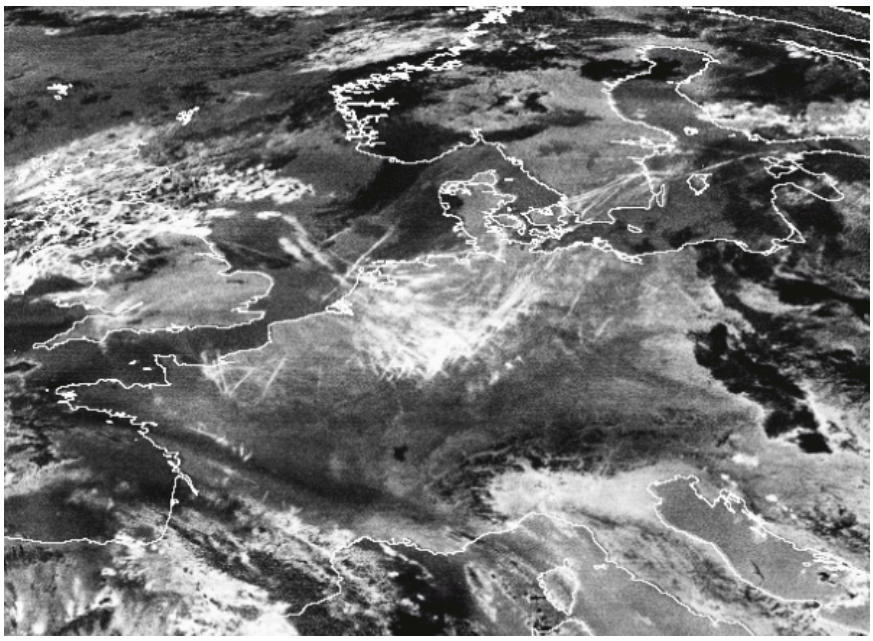

From EUMETSAT image library.

DO CONTRAILS SEEK CLEAR SKIES?

BACHELOR THESIS, 15 P.

Supervisors:
Johannes K. Nielsen, DMI
Elna Heimdal Nilsson, LU

The front-page image is obtained from EUMETSAT image library, showing 5 September 2004 12:01 UTC.

Abstract

Contrails are the visible line-shaped clouds that can be seen to form behind aircrafts if the air is saturated with respect to liquid. Furthermore, if the air is supersaturated with respect to ice, the contrails can develop into contrail-cirrus that affect the radiative forcing, locally up to an annual average of 1000 mWm^{-2} over Europe. Central Europe is especially exposed to contrails due to the frequent aviation and also because of trajectories drifting in towards central Europe from the North Atlantic. Previous results showing that contrails drift towards clear skies are confirmed by analyses of the mean radiances and trajectory movement, for initial random starting points over central Europe both for two individual months and three months combined. By time-shifting the initial starting points of the two individual months the possible reasons for the phenomenon are discussed. The increase of radiance along the trajectories might either be due to convective areas that push the trajectories toward areas of descending air or it might be due to the fact that the general tendency is drifting towards east where it normally is clearer skies.

Sammanfattning

Flygplansmoln eller kondensstrimmor är de linje-formade moln som formas bakom flygplan om luften är mättad med avseende på vatten. Om luften dessutom är mättad med avseende på is så kan kondensstrimmorna utvecklas till slöjmoln. Dessa moln påverkar strålningsbalansen, lokalt upp till 1000 mWm^{-2} per år över Europa. Över Centraleuropa är kondensstrimmor vanligt förekommande på grund av tät flygplanstrafik men också på grund av att trajektorier från Nordatlanten driver in. Tidigare resultat som visar att kondensstrimmorna driver mot molnfria områden är bekräftade av analyser på strålningen och trajektorierna. Analyserna är utförda för slumpmässiga startpunkter över centrala Europa samt för en tids-randomisering av startpunkterna. Detta utförs för två individuella månader och tre månader kombinerat. Genom att skifta tiden för startpunkten på de två individuella månaderna så kan möjliga orsaker till fenomenet att de söker sig till molnfria områden diskuteras, antingen är det på grund av konvektiva områden som stöter bort trajektorierna mot områden med sjunkande luft eller så är det på grund av de generellt driver mot öst där det i större utsträckning är molnfritt.

Acronyms

CCN	Cloud condensation nuclei
ECMWF	European Centre for Medium-Range Weather Forecasts
GFS	Global Forecast System
IR	Infrared
PBL	Planetary Boundary Layer
RF	Radiative forcing
RH	Relative humidity
TOA	Top of atmosphere
WV	Water vapour

Acknowledgements

This study has been performed with great help from Johannes K. Nielsen at the Danish Meteorological Institute who provided me with MATLAB-programs and data to use for the analyses. I am also grateful for the inspiration, suggestions and help with interpretation and discussion of the results as well as the effort of introducing me to Linux.

I would also like to thank Elna Heimdal Nilsson at Lund University for the support and help with my bachelor project and the critical evaluation of this paper.

Table of contents

1. Introduction

Aviation is often mentioned as one major agent in the prevailing climate change and global warming, not only due to the exhaust of greenhouse gases. The visible clouds that can be observed to form behind aircrafts are so called contrails and these might have a noticeable impact on the climate due to the effect on the Earth's radiative balance, according to Screen and MacKenzie (2004). Schumann (2005) suggests that the most important factors that affect the radiative forcing are the cloud cover and the optical depth of the cloud. Figure 1, from IPCC (2013), shows the radiative forcing from contrails on a global scale between 1980 and 2011. The effect of contrail-induced cirrus, which can be seen in the figure, will also be important in the discussion of this paper.

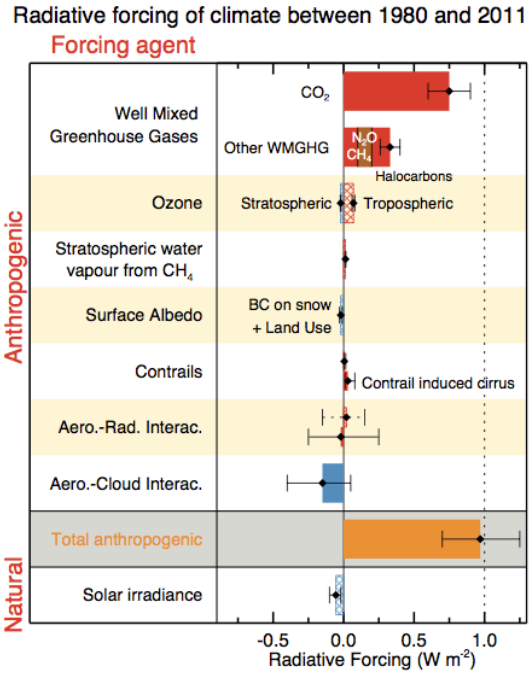

Figure 1. *The annual average radiative forcing globally from different forcing agents between 1980 and 2011. As can be observed, contrails give a very small contribution to the radiative forcing while contrail-induced cirrus are of more importance. (IPCC, 2013)*

Previous analyses performed by Nielsen (2009) show that there is an increased radiance along the trajectories of exhaust plumes for the first 20-30 hours after emission. The suggested explanation to this, by Nielsen (2009), is that the trajectories seem to drift toward clear sky areas where the radiance is higher. It is not clear what causes this phenomenon but one explanation by Nielsen (2009) is that convective areas on the surface cause a diverging wind field aloft. This diverging wind field will push the trajectories towards non-convective areas. The phenomenon could influence the climate impact of the contrails by giving rise to local effects, which makes it interesting to investigate further.

The aim of this study is to confirm or reject the previous results showing an increase of radiance with time along air trajectories over central Europe and to discuss possible reasons for this phenomenon. Also the climate impact of contrails will be discussed.

2. Background

2.1 Contrail formation

The formation of contrails can be explained by a thermodynamical theory entitled the Schmidt/Appleman criterion. The complete derivation of the theory has been performed by Schumann (1996) and a shortened version of it follows here.

One approximation in the theory is that the temperature of the plume of exhaust gases at the point of contrail formation is directly related to the specific enthalpy of the plume (Schumann, 2000). This approximation implies that the mixing amongst the plume and environmental air follows a straight line in a $(q - h_p)$ - diagram where q is the water vapour mass concentration and h_p is the specific plume enthalpy (Schumann, 2000). The water vapour mass concentration is related to the partial water vapour pressure e in an ideal gas as:

$$\frac{e}{p} = q\frac{R_{air}}{R_{H_20}} = \frac{q}{\varepsilon} \tag{1}$$

where p is the pressure and R refers to the gas constants of air and water, giving $\varepsilon = 0.622$ (Schumann, 2000).

Another reasonable approximation according to Schumann (2000) is that for a constant specific heat capacity of the air at constant pressure, c_p, the internal enthalpy of the air h and the temperature T are linearly related. This approximation means that the mixing line is nearly straight in a $(e - T)$ – diagram (that can be seen in Figure 2) where the slope of the line is determined by the parameter G:

$$G = \frac{\Delta e}{\Delta T} = \frac{p \cdot c_p \cdot \Delta q}{\Delta h \cdot \varepsilon} \tag{2}$$

The parameter G describes the ratio between changes in water vapour pressure and temperature during mixing between the environmental air and the plume of exhaust gases (Schumann, 2000).

From G, Schumann (2000) derives the threshold temperature T_M, which is the minimum temperature of the environmental air that is required for contrail formation (point M in Figure 2), for 100 % relative humidity (RH) in the environmental air from:

$$\frac{de_{sat}(T_M)}{dT} = G \tag{3}$$

where e_{sat} is the water vapour saturation pressure over liquid water. Furthermore, when RH ≠ 100 % in the environmental air, the threshold temperature T_C is obtained from:

$$T_C = T_M - \frac{e_{sat}(T_M) - RH \cdot e_{sat}(T_C)}{G} \quad (4)$$

The threshold temperature is shown as a mixing line in Figure 2 as the dashed line with end-point at C. The dashed line with end-point at E is the mixing line for the environmental temperature. Steeper lines imply a higher threshold temperature (Schumann, 2000). The curved full line shows the saturation-curve for liquid water and the curved dashed line refers to the saturation-curve with respect to ice. It is when the mixing lines penetrate the liquid saturation-curve that contrails can form, which means that the plume gases are saturated with respect to liquid water. For a standard atmosphere these conditions are met between 8.4 and 14 km (Schumann, 1996 and 2000).

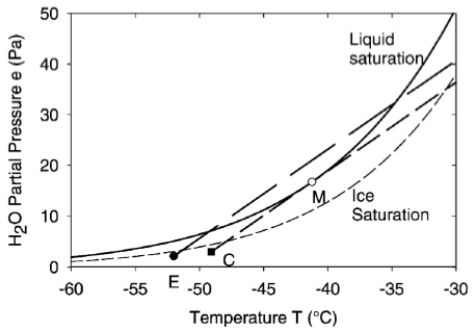

Figure 2. *A diagram of partial water vapour pressure, e, and temperature, T. The dashed lines are the mixing lines of environmental temperature (end-point at E) and of threshold temperature (end-point at C). The gradient of the mixing lines is obtained from the parameter G. Point M refers to the maximum of relative humidity during the mixing of environmental air and the exhaust plume under threshold conditions. (Schumann, 2000)*

The derivation by Schumann (1996) of the parameter G is based on the fact that aviation fuel consists mainly of hydrogen and carbon, which results in EI_{H_2O} mass units of water vapour per mass unit of fuel. This is referred to as the emission index for water vapour. Q is the specific combustion heat from the engine where a part of Q; η, is used to propel the aircraft.

From this, G can be rewritten as:

$$G = \frac{EI_{H_2O} \cdot c_p \cdot p}{\varepsilon \cdot Q(1-\eta)} \quad (5)$$

which indicates that the overall efficiency, η, of the engine is an important factor regarding contrail formation (Schumann, 1996). If η is increased, G will be steeper and that implies a higher threshold temperature. A higher threshold temperature leads

to an increased possibility of contrail formation at higher environmental temperatures and the consequence of that is that they can form at lower altitudes, according to Schumann (2000).

2.2 Persistent contrails and contrail-cirrus

If the ambient air is too dry the contrails will be very short-lived due to mixing with the dry air. But if the ambient air is supersaturated with respect to ice the particles in the exhaust plumes can form freezing nuclei and the contrails will then be persistent, according to Schumann (2000). Burkhardt and Kärcher (2011) state that there is a higher ice supersaturation frequency in colder areas, but in the cold air the water content in the air is low. Furthermore, this means that even though the thermodynamic conditions are met for contrail formation, the contrails are less likely to obtain a significant optical depth according to Burkhardt and Kärcher (2011).

Minnis et al. (1998) found that if there is ice supersaturation, the contrail particles will grow from small to larger crystal-size particles that normally do occur in naturally cirrus clouds. In a 2-year study in Lancaster by Screen and MacKenzie (2004) it was found that 61 % of all observed contrails were persistent and about 59 % of the contrails did spread out from the straight-line appearance and covered larger areas of the sky. According to Schröder et al. (2000), the particles grow from 1 µm to about 8 µm in an hour and during this time, the plume of exhaust gases dilutes with the environmental air causing a decrease in crystal concentration of about three orders of magnitude. The different stages in this process are shown in Figure 3.

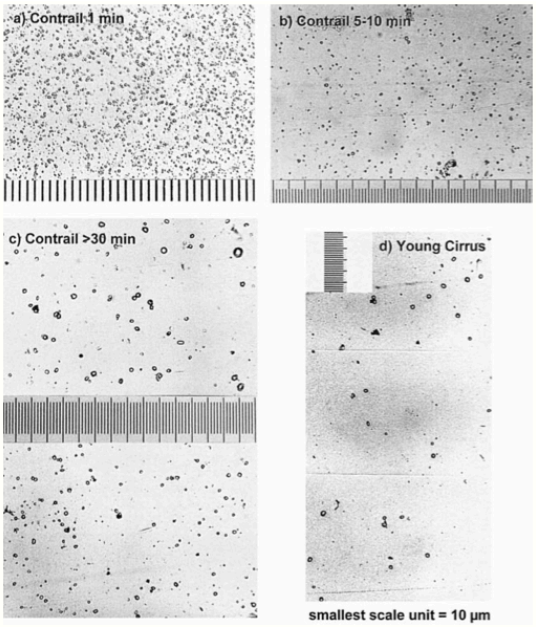

Figure 3. *a) A particle sample of a 1 min old contrail, b) after 5-10 min, c) after 30 min and d) a particle sample of the formed contrail-cirrus cloud. (Schröder et al., 2000)*

Analyses made by Mannstein and Schumann (2005) indicate that the contrail-cirrus coverage over central Europe is about 10 times higher than the coverage of pure contrails. Contrail-cirrus covered 3 % of the Earth's surface and the mean contrail coverage for the same period and area was estimated to be 0.3 %. Over Europe, Burkhardt and Kärcher (2011) found that the contrail coverage reached 2 % while the contrail-cirrus cover up to 10 %, which is the highest value obtained globally. According to Burkhardt and Kärcher (2011) this is because old contrails that form over the North Atlantic are advected into the central part of Europe.

According to Minnis et al. (1998) there exists a lot of ice supersaturated air that does not produce clouds due to the absence of condensation nuclei (CCN). The exhaust gases from airplanes will contribute with CCN and enable an anthropogenic cloud formation. From the results of the study by Minnis et al. (1998) it is also clear that contrail-cirrus do have a climate impact, at least on a regional scale. The effect of CCN can be referred to as indirect climate effect while the formation of contrails is a direct climate effect according to Sassen (1997). Sassen (1997) also suggests that contrail-cirrus may cover much larger areas than naturally occurring cirrus, because they can occur in areas where cirrus normally cannot form.

2.3 Climate impact

In an area with long-lived contrails and contrail-cirrus that have dispersed a lot, the largest impact on climate is due to the changes in the Earth's albedo, which affects the radiative balance according to Screen and MacKenzie (2004). Sassen (1997) explains that the newly formed contrails are optically dense and scatter the incoming solar radiation, even leaving shadows on the ground. Furthermore, he states that these contrails have a cooling effect of the Earth's surface, which is the opposite of an increased amount of cirrus clouds.

Meerkötter et al. (1999) explain that the radiative forcing (RF) at the top of the atmosphere (TOA) is strongest and positive during nighttime and if the optical depth is small the RF will be positive even during daytime. According to Meerkötter et al. (1999) the daily mean RF from contrail-cirrus at the top of the Earth's atmosphere is 0.11 to 0.13 Wm^{-2} if the optical depth varies between 0.2 and 0.5 and if the contrail-cirrus cover is about 0.1 %. Furthermore, Burkhardt and Kärcher (2011) state that the RF from contrail-cirrus on a global scale is approximately nine times larger than the RF from contrails. Over central Europe the net RF from contrail-cirrus is estimated to be more than 300 mWm^{-2} per year and globally, they estimate the net RF from contrails and contrail-cirrus to be 37.5 mWm^{-2} per year. According to Chen and Gettelman (2013) the local RF can reach up to an annual average of 1000 mWm^{-2} over the western parts of Europe. Furthermore, these high regional and local values of RF play a significant role compared to long-lived anthropogenic greenhouse gases, as can be seen in Figure 1 from IPCC (2013).

When assessing this topic, it is important to take the rather long (hourly timescale) lifetime of contrail-cirrus into account since the radiance will change through the course of the day, see Mannstein and Schumann (2005). During daylight there is a cooling effect of the enhanced reflection by the contrail-cirrus clouds, which balances the capture of infrared radiation from Earth quite well according to Mannstein and Schumann (2005) and during nighttime there will only be the warming effect from the capture of infrared radiation. Furthermore, most of the air traffic occurs during daytime over Europe, but the effect is transferred towards nighttime due to the delay of contrails transforming into contrail-cirrus. Also Chen and Gettelman (2013) point out the importance of the diurnal cycle of flights for the radiative effects, especially concerning the negative shortwave RF because it will not occur during nighttime when there is no solar radiation. Furthermore, the intensity of the shortwave radiation is dependent of the solar zenith angle but the longwave radiation does not differ so much during the day.

According to Burkhardt and Kärcher (2011), another climate impact following from contrail appearance is that they will change the water budget in the atmosphere. The effect is that naturally occurring clouds will not be able to form or develop when the water deposits on the ice particles in the contrail-cirrus. This will reduce the optical depth of existing clouds by up to 10 % or even replacing them entirely, which will reduce the direct climate effect of contrails.

3. Method

3.1 Parcel trajectories

In a MATLAB-script made by Nielsen (2009) the parcel trajectories are started from randomly selected points over central Europe between 9 and 11 km altitude in a time frame of a month. About 10 new trajectories are started each 0.25 hour (no diurnal dependence) and followed until they leave the simulation box. In order to calculate the parcel trajectories, central Europe is approximated as a simulation box with a flat surface at latitude 41° - 59°N, longitude 1° - 19°E and an altitude between 4 and 19 km. This box consists of grid boxes with $29 \times 30 \times 17$ grid points. The wind field data used in the calculations is obtained from ECMWF reanalysis of 40° - 60°N, 0° - 20°E and altitude levels 14-46 that corresponds to a pressure of 10 – 750 hPa, for each month. The wind field is interpolated on the grid boxes of the simulation box and the forward trajectories are calculated with second order Runge-Kutta and interpolation between the grid points. This gives an array of coordinates for the parcels that describe the trajectories, which are shown in Figure 4.

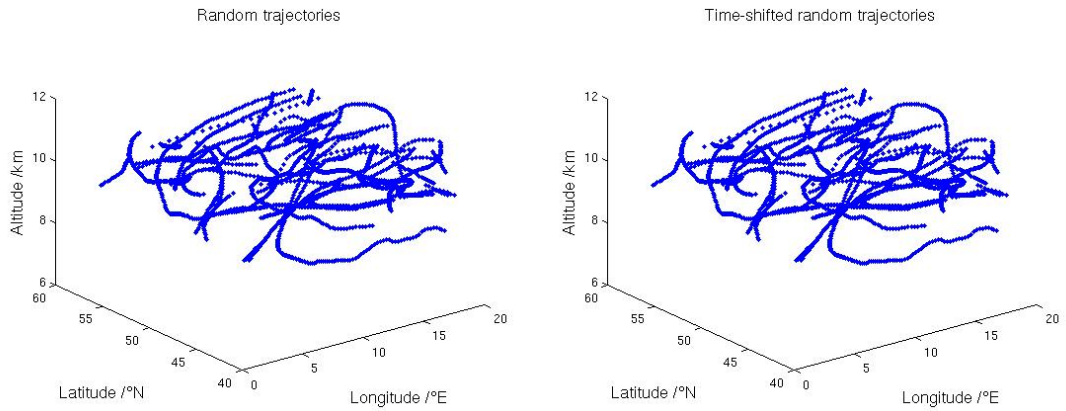

Figure 4. *The calculated randomly selected trajectories with initial random starting point (left) and time-shifted randomized starting point (right) for September 2005.*

To find out the tendency of the trajectory movement, an addition to the existing code was performed within the project in order to plot the average change along the longitude with time and the average change along the latitude with time. See Appendix A for the additional code. This should verify that that the trajectories drift eastward. In order to see if the explanation to the enhanced radiance is due to the general tendency of the trajectories drifting eastward where it normally is clearer skies (higher radiance), which can be seen in Figure 5, a random time-shift of the initial randomly selected trajectories is also made within the project. Adding a randomizing function to the existing code does the random time-shift, see Appendix B for the addition.

Randomizing the trajectories means that they get a new time starting point in the analyses compared to their initial time starting point, but the actual spatial coordinates will in the end be the same, as seen in Figure 4. If the results from this time-shift resemble the initial results in the analyses, the eastward drifting might be one explanation to the phenomenon that trajectories and contrails drift towards clear skies.

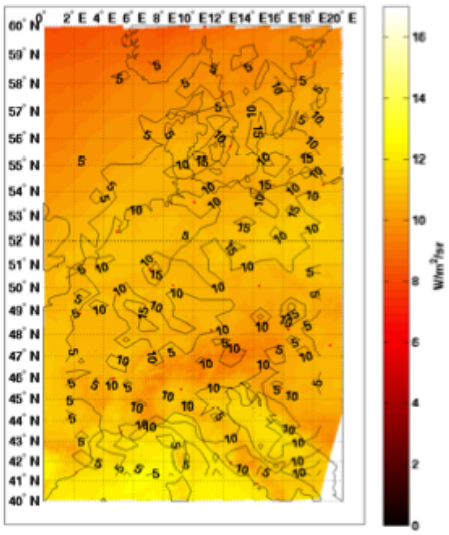

Figure 5. *The mean radiance obtained from IR-images by Meteosat 7 for September 2005. Only the colour scale is of relevance here, where yellow colours indicate higher radiance compared to red colours. (Nielsen, 2009)*

3.2 Satellite images

The parcel trajectories are correlated with satellite images that are recorded every 30 minutes from the geostationary satellite Meteosat 7, in order to investigate the radiance for each of the months. The data were downloaded from EUMETSAT on a 2500 × 2500 pixel grid. One IR-channel at 10-13 µm and one WV-channel at 5.5-7.2 µm are used in the analyses. The radiance in each trajectory-pixel is counted by transforming the trajectory coordinates into pixel indexes. A software program for unpacking and converting coordinates of the satellite images into pixels is included in the code made by Nielsen (2009) that handles the Open MTP format used by EUMETSAT.

3.3 Analyses

The analyses are performed for the individual months October 2004, which have not been done before, and also for September 2005 for both the initial random starting points and the randomly time-shifted starting points to be able to compare the results. The comparison is done in order to see if the enhanced radiance with time is due to the eastward drifting or due to convective areas, or maybe both.

In the analyses of the individual months the mean radiance of the trajectories is determined each half-hour along with the radiance of the trajectories at their starting points. For comparison, the mean radiance from the whole investigated area will also

be analysed from the satellite images each half-hour. This comparison will show whether the radiance is increased or not along the trajectories, by plotting the radiance relative to time. Some defected radiance values are moved out manually from the analyses. By plotting the mean radiance of the trajectories relative to their initial radiance, in both space and time, relative to their age will show the time dependence of radiance. This relative radiance will also be analysed for three different months combined, September and October 2004 and September 2005. The written code for this can be found in Appendix C. To see how the trajectories' movement tendencies appear, the average altitude, longitude and latitude of the trajectories with time are also investigated for the individual two months.

The unit for the radiance is $Wm^{-2}sr^{-1}$, where sr refers to steradian, which is a dimensionless SI-unit that is also known as solid angle. One can imagine a cone with the top referring to the radiating point at the Earth's surface and the bottom referring to the area detected by the satellite.

3.3.1 Computation of errors

The error-bars shown in Figures 10-18 are due to variability in the radiance from the satellite pictures. A problem with calculating the errors is that the individual trajectories are not completely independent of each other; in fact they are to some degree correlated. To be able to use the Gaussian error propagation of uncertainties the trajectories need to be independent. So the errors are estimated with help of an auto-correlation function for the longitudinal distance that is determined from the satellite images. For the latitudinal auto-correlation one important factor is the north to south climatic gradient, which makes it a bit more difficult to calculate and gives a more inexact result.

For each trajectory the variance of radiance is σ_{Ra}^2 and the error-bars are calculated as $\sqrt{\sigma_{Ra}^2/N}$, where N is the number of days in the analyses, 30 days for the individual months and 90 days for the three months combined. This is because it is only possible to assume that there is one independent measurement of radiance per day, as can be seen in Figures 10-14 that show how the de-correlation of the trajectories first starts after 20-40 hours.

4. Results and discussion

4.1 Do contrails seek clear skies?

4.1.1 Radiance for two individual months

Figures 6-9 show the mean radiance of the trajectories and the mean radiance of the whole area. In Figures 6-7, which refer to the initial random starting point, it can quite clearly be seen that the radiance is increased along the trajectories by comparing the red and blue lines where the blue line is the mean radiance of the trajectory and the red line is the mean radiance of the area. These results indicate that the trajectories drift towards areas with higher radiance for both October 2004 and September 2005.

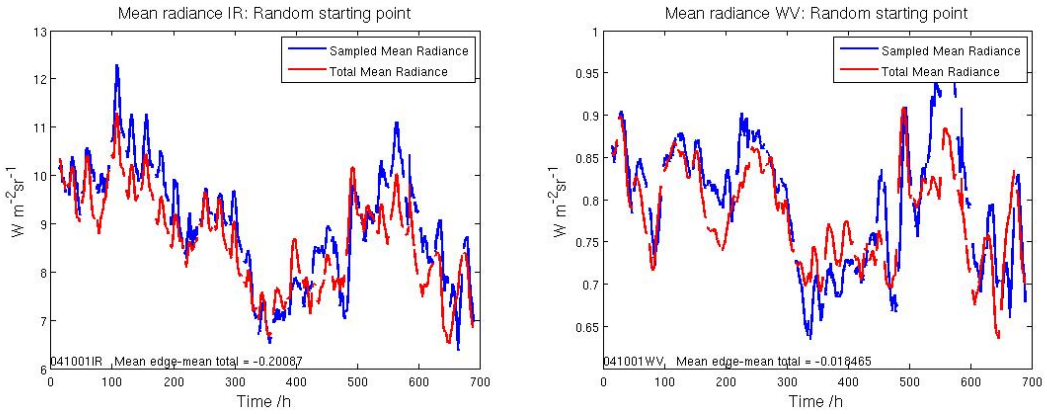

Figure 6. *The mean radiance recorded along the trajectories with initial starting points (blue line) compared with the mean radiance of the whole investigated area (red line). Left: IR analyses. Right: WV analyses. For October 2004.*

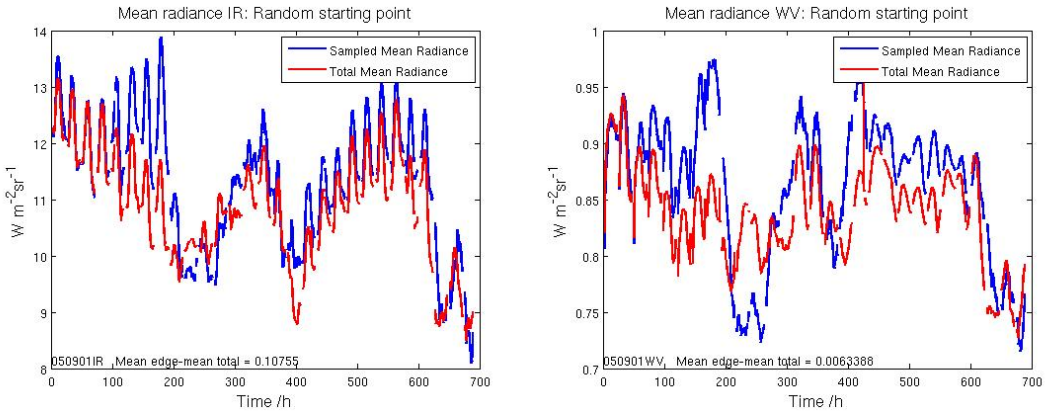

Figure 7. *The mean radiance recorded along the trajectories with initial starting points (blue line) compared with the mean radiance of the whole investigated area (red line). Left: IR analyses. Right: WV analyses. For September 2005.*

When the initial starting points are randomized in time, shown in Figures 8-9, the enhanced radiance along the trajectories cannot be seen. Actually, for October 2004 in Figure 8 the opposite result is found, namely decreasing radiance along the trajectories.

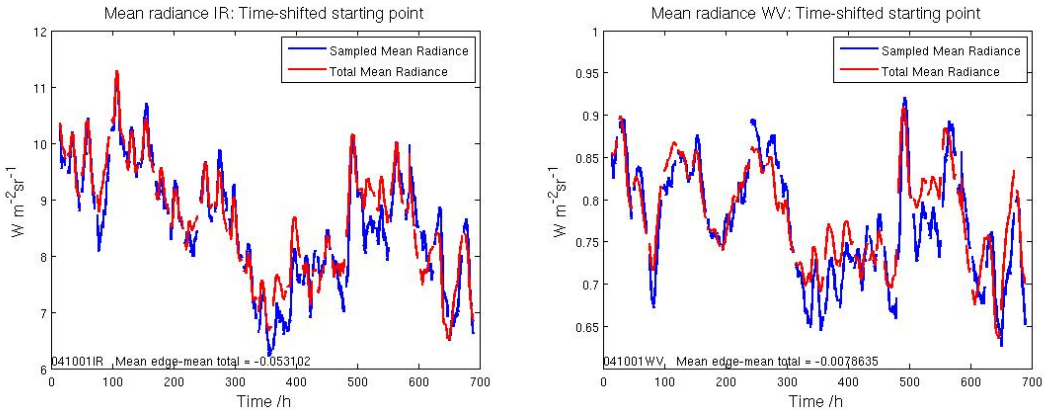

Figure 8. *The mean radiance recorded along the trajectories with time-shifted starting points (blue line) compared with the mean radiance of the whole investigated area (red line). Left: IR analyses. Right: WV analyses. For October 2004.*

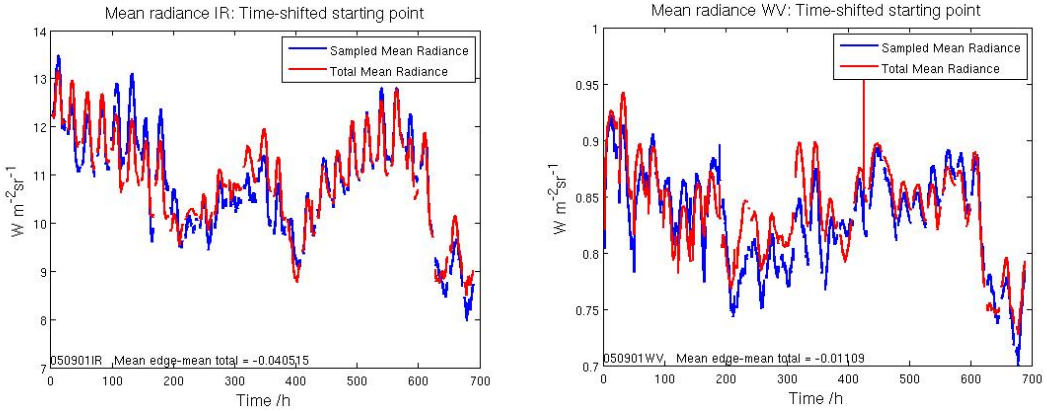

Figure 9. *The mean radiance recorded along the trajectories with time-shifted starting points (blue line) compared with the mean radiance of the whole investigated area (red line). Left: IR analyses. Right: WV analyses. For September 2005.*

For September 2005 however, the radiance along the trajectories is agreeing quite well with the mean radiance of the whole simulation area. The agreement of the mean radiances imply that the random time-shift of the trajectories do work and the explanation to the result is that some of the trajectories will be started in areas where there are higher radiance and some of the trajectories will be started so that they reach areas with lower radiance, which for example are in convective low-pressure areas.

In Figure 10 it can be seen how the radiance increases along the initial random trajectories with time, for October 2004. The analyses for October 2004 only run up to about 80 hours due to the fact that there are no trajectories followed longer than

that, but for September 2005 they are followed up to 100 hours. The same result of increasing radiance along the trajectories is also found for September 2005, in Figure 11.

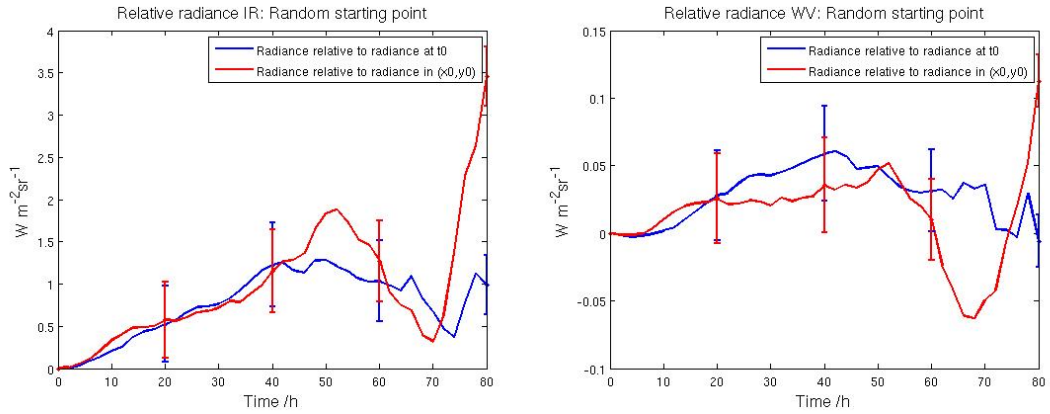

Figure 10. *The mean radiance of the initial random trajectories relative to the radiance at their starting points. The blue line is relative to the time starting point and the red line is relative to the spatial starting point. Left: IR analyses. Right: WV analyses. For October 2004.*

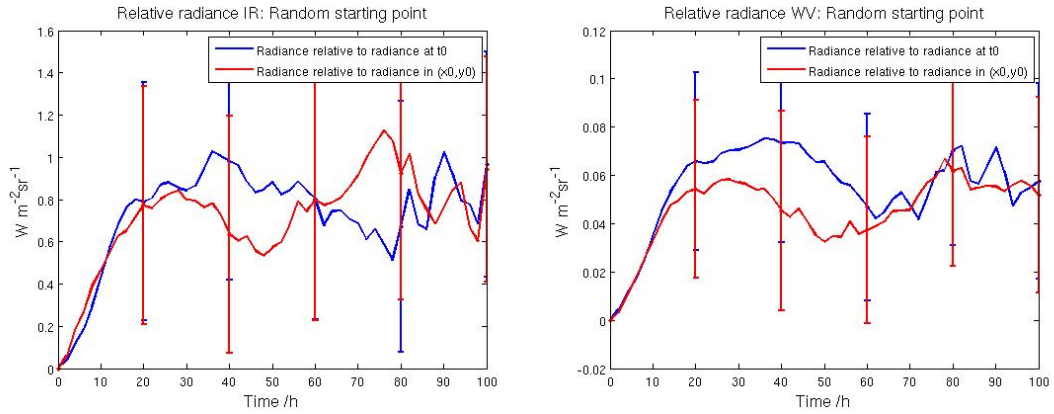

Figure 11. *The mean radiance of the initial random trajectories relative to the radiance at their starting points. The blue line is relative to the time starting point and the red line is relative to the spatial starting point. Left: IR analyses. Right: WV analyses. For September 2005.*

In Figures 12-13, after time-shifting the trajectories starting point, the radiance is clearly averaged out. The relative radiance is just alternating around zero and showing no tendency of increasing or decreasing, except for October 2004 where it is a large fluctuation after 60 hours that probably is due to the fact that there is to few data points at the end since not many trajectories are followed for so long time. This is in quite good agreement with the results shown in Figure 8 and 9 where there are no signs of increased radiance along the trajectories.

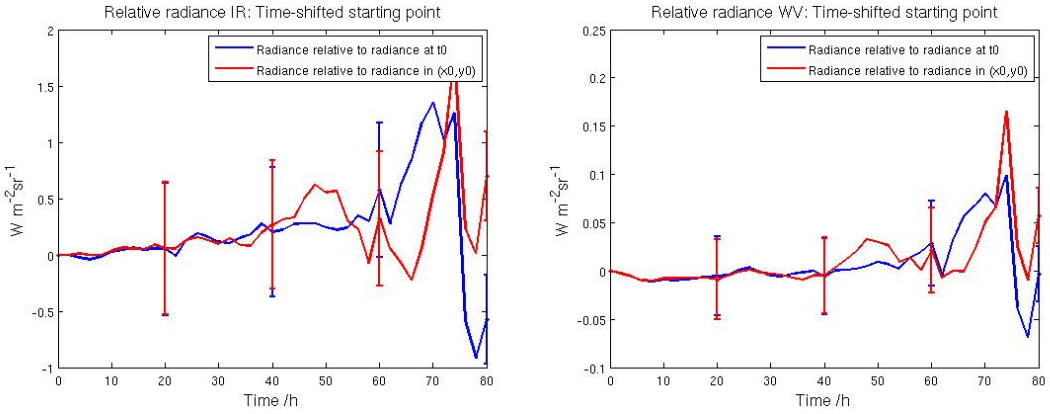

Figure 12. *The mean radiance of the random time-shifted trajectories relative to the radiance at their starting points. The blue line is relative to the time starting point and the red line is relative to the spatial starting point. Left: IR analyses. Right: WV analyses. For October 2004.*

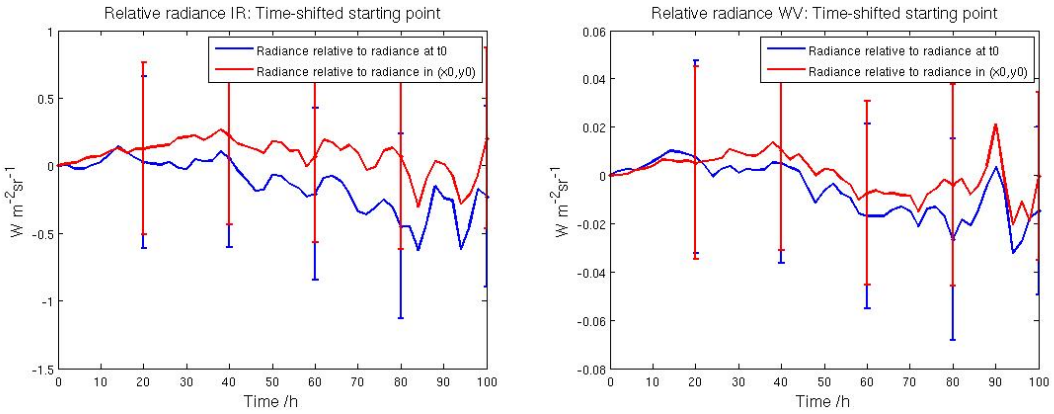

Figure 13. *The mean radiance of the random time-shifted trajectories relative to the radiance at their starting points. The blue line is relative to the time starting point and the red line is relative to the spatial starting point. Left: IR analyses. Right: WV analyses. For September 2005.*

From these results it is possible to say that eastward drifting towards areas with higher radiance is not the cause for the enhanced radiance along the trajectories with time because then the random time-shift would not be of relevance. Instead the local effect of divergence above convective areas seems to be a much more important factor of the phenomenon.

4.1.2 Radiance for three months

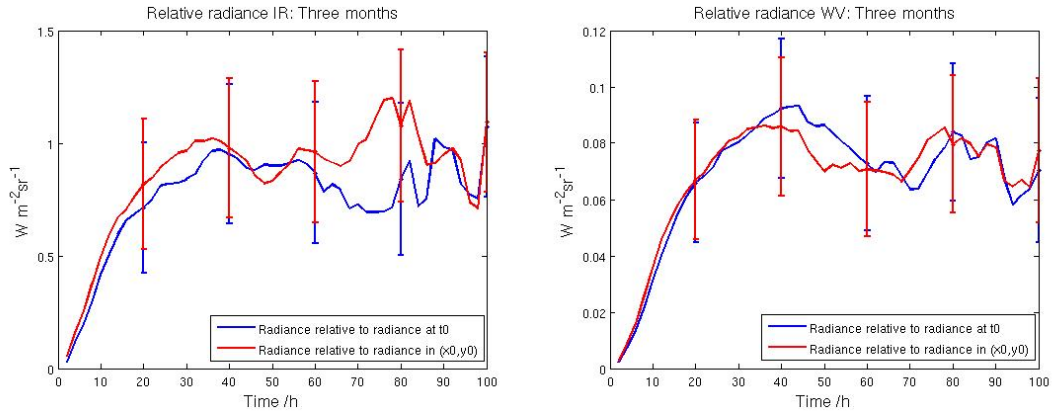

Figure 14. *The mean radiance of the initial random trajectories relative to the radiance at their starting points. The blue line is relative to the time starting point and the red line is relative to the spatial starting point. Left: IR analyses. Right: WV analyses. For the three months September 2004, October 2004 and September 2005.*

The result of the three months combined is shown in Figure 14 and indicates that the radiance along the trajectories increases for the first 40 hours. The result seems very reasonable when it is compared with the result for the two individual months in Figure 10 and 11, since it is between the estimated uncertainties. The fact that the radiance along the trajectories becomes saturated after a while indicates that the trajectories remain in clear sky areas.

This resembling result gives further confirmation to the previous results found by Nielsen (2009). It can also be seen in Figure 14 how the error-bars are smaller since there are more days in the analyses, which makes the result trustworthier. So this result is actually strongly confirming the theory that contrails drift towards clear skies and show that it is not only due to a specific phenomenon during a short period of time.

4.1.3 Trajectory altitude, longitude and latitude

The altitude change of the trajectories with time correlates well for the initial random starting points and the randomly time-shifted starting points, as can be seen in Figures 15-16. The resembling results are correct, because when averaging the altitude by taking the initial altitude away from the actual altitude of the trajectories the time starting point is of no relevance. The small change in appearance is probably due to the approximative model. However, the altitude change of the trajectories with time does not correlate between October 2004 and September 2005. For October 2004 the altitude increases, as can be seen in Figure 15, while it decreases for September 2005 that can be seen in Figure 16.

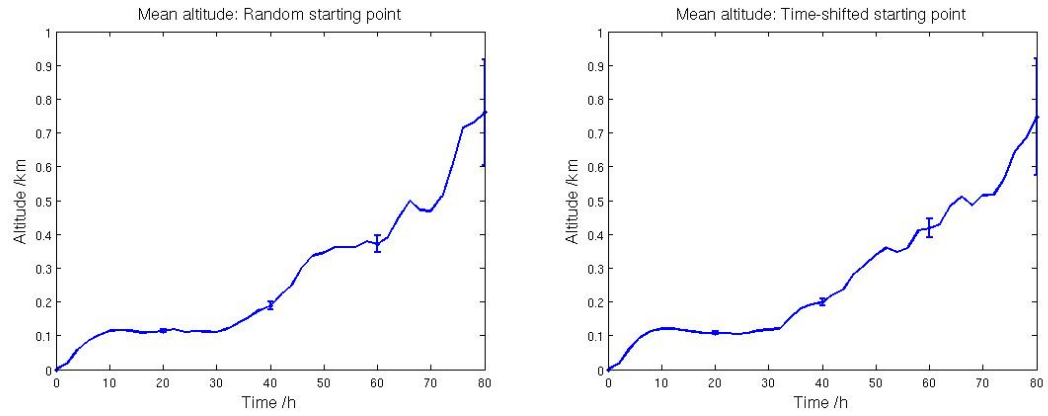

Figure 15. *The average change in altitude of the trajectories with their age for October 2004. Left: For the initial random starting point. Right: For the randomly time-shifted starting point.*

The increasing altitude does not agree well with the theory that the trajectories drift away from convective areas, rather towards them.

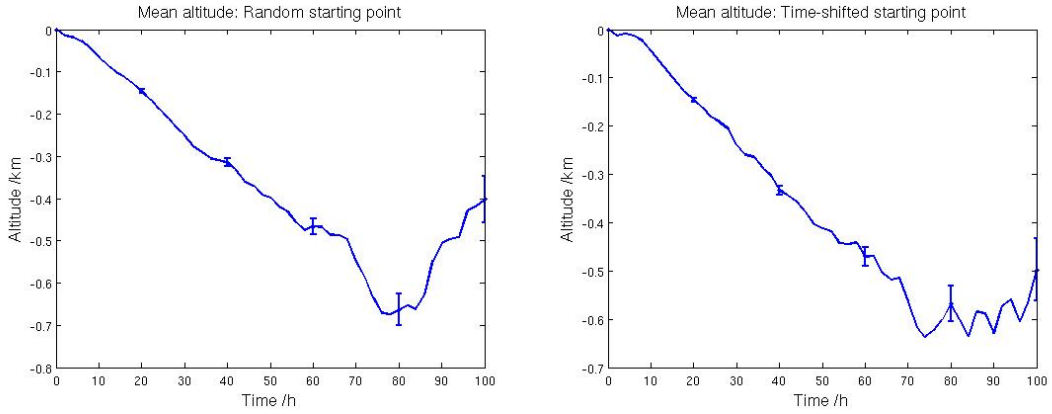

Figure 16. *The average change in altitude of the trajectories with their age for September 2005. Left: For the initial random starting point. Right: For the randomly time-shifted starting point.*

The decreasing altitude of the trajectories in September 2005 might indicate that the trajectories drift away from local convective areas with upper level divergence, which means that they are pushed towards areas of descending air. Descending air areas are associated with high pressure at the ground and areas of rising air are correlated with lower pressure at the ground.

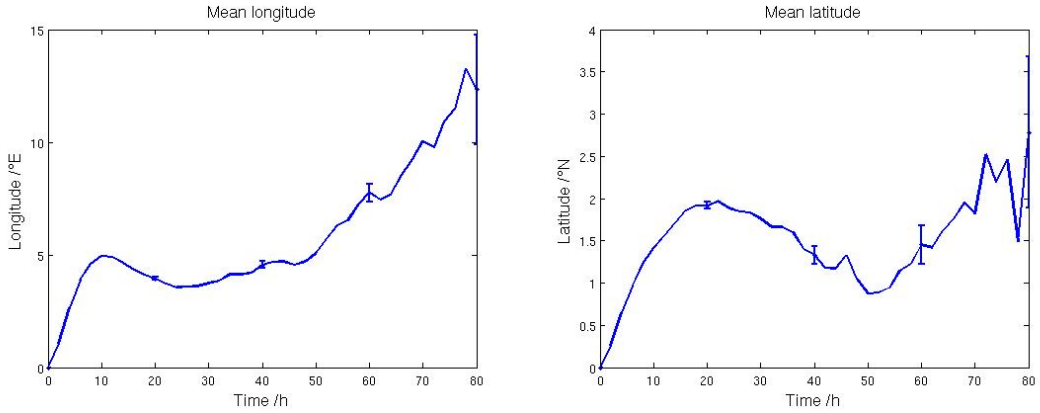

Figure 17. *The average change in longitude (left) and latitude (right) of the trajectories with their age. For October 2004.*

The average change in longitude and latitude for October 2004, shown in Figure 17, clearly indicates that the trajectories drift towards east as the longitude is increasing with time. For October 2004 the average latitude of the trajectories also increases, although very little, meaning that they drift slightly to the north as well.

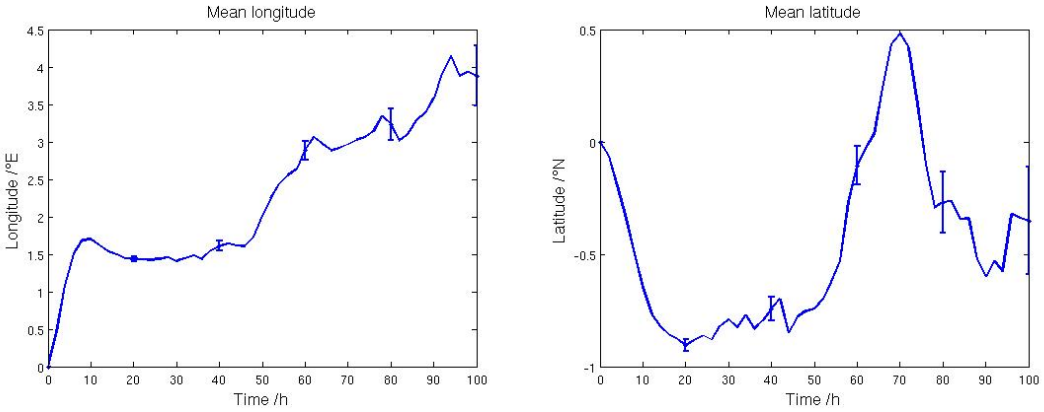

Figure 18. *The average change in longitude (left) and latitude (right) of the trajectories with their age. For September 2005.*

In Figure 18 the average change in longitude and latitude of the trajectories in September 2005 can be seen. As in October 2004, also these results clearly indicate that the trajectories drift eastward. The increment of latitude cannot be seen for September 2005. The longitude and latitude analyses were made only for the initial random points because the time-shifted trajectories will resemble this result just as the average altitude change of the trajectories, as seen in Figures 15-16.

4.1.4 Limitations of the analyses

It is not so convenient to make any conclusions out of just two different months with data. It is known from the GFS archive (obtained from Wetter3) that September 2005 is quite dominated by high pressure, except for some individual days with lower pressure. October 2004 however, seems to be more exposed to lower pressure according to my own observations, which possibly could explain the result of decreased radiance along the trajectories in Figure 8. The tendency of pressure might also explain the change in altitude, which decreases for September 2005 but increases for October 2004, as seen in Figures 15-16. Actually, this observation could also explain that the trajectories in October 2004 drift a bit towards north and leave the simulation box faster than in September 2005 as the low pressure systems coming in from west will cause the air over central Europe to move northward. In September 2005, which is more dominated by high pressure, the air will not move as much.

The analysis of the three combined months is one solution in order to get less impact from short-term specific weather phenomenon, but still it might be a problem that only September and October are analysed since they are in the same season. It is possible that another result would be obtained if the analyses were made at a different time of the year, when the air masses are somewhat different both in appearance and behaviour, generally with frequent lows coming in during fall and winter and greater chance of high pressure during spring and summer.

One limitation of the model is that it approximates central Europe as a flat homogeneous surface that is not narrowed with higher latitudes, which will affect the calculated positions of the trajectories to some degree. However, it should not have a significant effect on the result because the scale of convective areas is large compared to this error.

The large error-bars are somewhat exaggerated as a consequence of the difficulty to do the error computations with the auto-correlation function implying that only one independent trajectory each day is possible. It might be possible to have a few more independent trajectories each day and then obtain smaller error-bars.

4.2 The climate impact of contrails

4.2.1 Radiative forcing

It is clear that the radiative forcing of the atmosphere is affected by aviation. However, it is not clear how extensive the effect is. Even if the Schmidt/Appleman criterion is not fulfilled such that no formation of contrails occurs, there will be emission of aerosols, which can act as CCN and enhance the probability for cloud formation. But the most essential factor is of course the formation of contrails and especially contrail-cirrus. Over central Europe the RF plays a significant role in climate impact compared to long-lived greenhouse gases, according to Chen and Gettelman (2013), even if that is not the case on a global scale.

The RF is affected by the phenomenon that contrails drift towards clear skies and also remain there by the fact that more infrared longwave radiation will be captured during nighttime, which probably has the largest warming impact. During daytime, if the contrail-cirrus obtain a significant optical depth, this positive RF could be somewhat reduced because the contrail-cirrus will contribute with a negative RF compared to if there would have been clear skies.

4.2.2 Diurnal cycle and water budget

The diurnal cycle is shown to be important but it is not easy to take it into account if the objective is to decrease the climate impact of contrails over central Europe. If all the flights occurred during daytime when contrails might have a total negative RF, they would instead lead to the formation of contrail-cirrus during the evening and night. Since the contrail-cirrus is much more widespread than the contrails, the RF will be largely positive during nighttime. But if the flights only occurred during early morning the negative RF from the contrails would appear and the overall RF would probably not be largely positive due to the fact that the contrail-cirrus does occur during daytime but not during nighttime. Except that these restricted flight times would not be possible in our global world where people are dependent on aviation, the problem also seems to be that it is not only the actual flights over central Europe that are contributing with contrails. Because of the westerlies, contrails from the North Atlantic will move in over Europe and to some extent accumulate, which also is shown in Figures 17-18. But according to Burkhardt and Kärcher (2011) it is possible that the contrail reduces the formation of naturally occurring clouds so much, by using most of the available water in the atmosphere, that the radiative forcing will be less positive. However, Sassen (1997) implies that there maybe would not exist clouds that would capture longwave radiation in these areas at all without sufficient amount of CCN that comes along from the aircraft exhaust.

4.2.3 Air masses

The most interesting thing to discuss in relation to the climate impact is probably the flight level and air masses. For example, cold air masses are less likely to produce contrail-cirrus of significant optical depth (they are so thin that they cannot be seen or detected by satellites) even though contrails can form, according to Burkhardt and Kärcher (2011). Remember that contrail-cirrus cover about ten times larger areas over central Europe than contrails do and also contribute with nine times larger positive RF, so it is contrail-cirrus that are most meaningful when discussing climate and global warming. Meteorological services could possibly guide the air traffic to dry and cold air masses to some extent, where the environmental air is not ice supersaturated. Also the flight level could be adjusted to avoid air masses that are supersaturated with respect to ice so that contrail-cirrus will not be able to form and the positive RF would be default during nighttime.

Since the results of this study indicate that the trajectories drift towards clear skies, maybe as a result of descending air as in September 2005, the cloud formation could possibly be completely default even if CCN is released within the exhaust gases because these clear sky areas are not favourable for cloud formation anyway. But on the other hand, if the flight would occur in an air mass where there already is extensive cloud formation, that is convective areas as Figure 15 is indicating for October 2004, the formation of contrails maybe would not change the radiative forcing that much anyway due to overlap with already existing clouds and change in the water budget.

5. Summary and outlook

The previous results of increased radiance along trajectories are confirmed, both for the two individual months and the three combined months, and the result obtained from time-shifting the starting points of the trajectories strongly suggests that the explanation to the phenomenon is that convective areas affect the trajectories and push them towards clear sky areas. It is shown that the trajectories drift towards east where it normally is clearer skies and higher radiance, but since the time-shifted trajectory starting points give a different result from the initial trajectory starting points, it cannot be the only explanation. However, it cannot be completely excluded since the results for October 2004 indicate that the trajectories are exposed to rising air that would imply cloud-covered skies, but still the trajectories have an increased radiance. According to my observations, the prevailing pressure tendency for the period seems to affect the height tendency of the trajectories.

The climate impact of contrails is very complex since it is dependent on so many different factors: contrail formation, contrail-cirrus formation, optical depth, diurnal cycle, CCN and so on. But the overall results indicate that there is a very high positive RF over central Europe due to the extensive air traffic. One reason for the high RF could also be the clear skies phenomenon since the contrails probably have a larger impact on the RF in that case.

Having knowledge about air masses and being able to forecast them would be of great advantage in order to avoid contrail formation, in combination with more understanding of how trajectories spread out.

A future approach of this work would be to investigate more data; longer time-series, another season and different areas of the Earth to see if the results will be confirmed or if it is just a regional phenomenon over central Europe due to the meteorological circumstances. The method should preferably be improved, for example making the simulation box more accurate and not as a flat surface and it would also be interesting to combine the results with actual flight patterns and not only random trajectories.

6. Self-reflection

During the process of this thesis I have gained knowledge about contrails that I did not have before, both about the thermodynamics behind the formation of them and the relevance of them in the climate debate. By reading lots of papers about the topic I have gained some understanding of the current research. I have also come to the insight of how little that is known today about the phenomenon since it is so complex to investigate, especially the effect of contrail-cirrus. I have explored the experimental part of it by running analyses myself to investigate the specific tendency that the contrails drift towards clear skies. Investigating this phenomenon with respect to climate also put this thesis in a context that is relevant for everyone and not only physicists.

As a physicist, I have gained more knowledge in modelling as well as the thermodynamics behind contrail formation. As a meteorologist, I have learned about a new feature that might impact the forecasting of cloud cover.

When doing the analyses I have critically evaluated the model and data. Even if the data is from ECMWF and EUMETSAT, which probably are some of the best places to gather this kind of data from I realise that it is still not perfect since I manually had to remove some defect values. I have chosen to use information from peer-reviewed papers in order to get correct information for the background section and also the discussion. Since the research of the subject is constantly evolved, I have also tried to find as newly published paper as possible that still have relevant information.

I am now more comfortable working in Linux, because of that I have learned some basic commands and seen the advantage of using it. My experience with MATLAB has also improved a lot and I have used problem-solving skills to write some code on my own to investigate a theory, but also to troubleshoot already existing code.

The thesis is written so that someone with my knowledge should be able to understand it and by writing the popular abstract I have also practised to write for the general public.

References

Burkhardt, Ulrike, Kärcher, Bernd. (2011), *Global radiative forcing from contrail cirrus, Nature Climate Change*, doi: 10.1038/NCLIMATE1068

Chen, C.-C., Gettelman, A. (2013), *Simulated radiative forcing from contrails and contrail cirrus,* Atmos. Chem. Phys., 13, 12525-12536.

IPCC. Myhre, G., D. Shindell, F.-M. Bréon, W. Collins, J. Fuglestvedt, J. Huang, D. Koch, J.-F. Lamarque, D. Lee, B. Mendoza, T. Nakajima, A. Robock, G. Stephens, T. Takemura and H. Zhang. (2013), *Anthropogenic and Natural Radiative Forcing. Climate Change 2013: The Physical Science Basis.* Contribution of Working Group I to the Fifth Assessment Report of the Intergovernmental Panel on Climate Change [Stocker, T.F., D. Qin, G.-K. Plattner, M. Tignor, S.K. Allen, J. Boschung, A. Nauels, Y. Xia, V. Bex and P.M. Midgley (eds.)]. Cambridge University Press, Cambridge, United Kingdom and New York, NY, USA.

Mannstein, H., Schumann, U. (2005), *Aircraft induced contrail cirrus over Europe*, Meteor. Z., 14, 549-554.

Meerkötter, R., Schumann, U., Doelling, D. R., Minnis, P., Nakajima, T., Tsushima, Y. (1999), *Radiative forcing by contrails*, Ann. Geophysicae, 17, 1080-1094.

Minnis, P., Young, D.F, Garber, D.P, Nguyen, L., Smith, W.L.Jr., Palikonda R. (1998), *Transformation of contrails into cirrus during SUCCESS*, Geophys. Res. Lett., 25, 1157-1160.

Nielsen, Johannes K. (2009), *Correlation of airplane emissions with Meteosat 7 IR/WV images,* Danish Meteorological Institute.
http://www.dmi.dk/fileadmin/Rapporter/DKC/dkc09-02.pdf (Access 25 March 2014)

Sassen, Kenneth. (1997), *Contrail-cirrus and their potential for regional climate change*, Bulletin of the American Meteorological Society, 9, 1885-1903.

Schröder, F., Kärcher, B., Duroure, C., Strom, J., Petzold, A., Gayet, J.-F., Strauss B., Wendling, P., Thomas, A. (2000), *On the transition of contrails into cirrus clouds*, J. Atmos. Sci., 57, 464-480.

Schumann, U. (1996), *On conditions for contrail formation from aircraft exhaust*, Meteor. Z., 5, 4-23.

Schumann, Ulrich. (2000), *Influence of propulsion efficiency on contrail formation*, Aerosp. Sci. Technol., 4, 391–401.

Schumann, Ulrich (2005), *FORMATION, PROPERTIES AND CLIMATIC EFFECTS OF CONTRAILS*, Aeronet.
http://aero-net.info/fileadmin/aeronet_files/links/documents/DLR/Schumann_Contrails.pdf
(Access 25 March 2014)

Screen, James A., MacKenzie, A. Robert. (2004), *Aircraft condensation trails and cirrus*, Weather, 5, 116-121.

Wetter3, Archiv-Version des Animationstools , GFS Analyse 500 hPa Geopotential, Bodendruck, Relative Topographi, http://www.wetter3.de/Archiv/index.html (Access 14 April 2014)

Front-page image from EUMETSAT image library for 05 September 2004 12:01 UTC, Meteosat-8.
http://www.eumetsat.int/website/home/Images/ImageLibrary/DAT_IL_04_09_05_C.html
(Access 16 April 2014)

Appendix A Trajectory movement

```
%%%Trajectory movement along longitude and latitude

%Longitude
x01=x00(:,1:2:end);
x1=x(:,1:2:end-1);
x1=x1.*I;
x01=x01.*I;

dx=x1-x01;
IX=ceil((ttt-t01)*3600/binsize)+1;
X=zeros(size(dx,2),1);
X2=zeros(size(dx,2),1);
NX=zeros(size(dx,2),1);
for i=1:size(dx,1);
    for j=1:size(dx,2);
        X(IX(i,j))=X(IX(i,j))+dx(i,j);
        X2(IX(i,j))=X2(IX(i,j))+dx(i,j)^2;
        NX(IX(i,j))=NX(IX(i,j))+1;
    end;
end;

figure(5)
clf

plot(((1:size(X,1))-1).*binsize/3600,X./NX,'linew',2);
hold on
eb0=errorbar(((1:10:size(X,1))-
1).*binsize/3600,X(1:10:end)./NX(1:10:end),sqrt(X2(1:10:end)./(NX(1:10:end).^2)),'.','
linew',2);
xlim([0 100]);
errorbar_tick(eb0);
title('Mean longitude')
xlabel('Time /h'),ylabel('Longitude /°E');

%Latitude
y01=y00(:,1:2:end);
y1=y(:,1:2:end-1);
y1=y1.*I;
y01=y01.*I;

dy=y1-y01;
IY=ceil((ttt-t01)*3600/binsize)+1;
Y=zeros(size(dy,2),1);
Y2=zeros(size(dy,2),1);
NY=zeros(size(dy,2),1);
for i=1:size(dy,1);
    for j=1:size(dy,2);
        Y(IY(i,j))=Y(IY(i,j))+dy(i,j);
        Y2(IY(i,j))=Y2(IY(i,j))+dy(i,j)^2;
        NY(IY(i,j))=NY(IY(i,j))+1;
    end;
end;

figure(6)
clf

plot(((1:size(Y,1))-1).*binsize/3600,Y./NY,'linew',2);
hold on
eb0=errorbar(((1:10:size(Y,1))-
1).*binsize/3600,Y(1:10:end)./NY(1:10:end),sqrt(Y2(1:10:end)./(NY(1:10:end).^2)),'.','
linew',2);
xlim([0 100]);
errorbar_tick(eb0);
title('Mean latitude')
xlabel('Time /h'),ylabel('Latitude /°N');
```

Appendix B Time-shifting starting points

```
randstart1=randperm(size(x,2))' %gives random starting point
randstart=randstart1(1:size(x,1));
moveindex=mod(randstart*ones(1,size(t00,2))+ones(size(t00,1),1)*(1:size(t00,2)),size(t
00,2))+1; %move trajectories to a new starting point
for i=1:size(x,1)
    movex(i,moveindex(i,:))=x(i,1:end-1); %new x-values
end

for i=1:size(x,1)
    movey(i,moveindex(i,:))=y(i,1:end-1); %new y-values
end

for i=1:size(x,1)
    movez(i,moveindex(i,:))=z(i,1:end-1); %new z-values
end

 movet00=zeros(size(t00));
for i=1:size(x,1)
    movet00(i,moveindex(i,:))=t00(i,:); %new t00-values
end

figure(1)
plot3(movex(1,:),movey(1,:),movez(1,:),'.')
title('Time-shifted starting point')
xlabel('Longitude /°E')
ylabel('Latitude /°N')
zlabel('Altitude /km')

s00=zeros(size(t00));

%overwriting x,y,z,t00 with random starting point
x=movex;
y=movey;
z=movez;
t00=movet00; %the values of t00 is not used any more - t00 serves as indexmatrix.
```

Appendix C Three months

```
filen='041001'
ext='L';
head
yy=filen(1:2);
mm=filen(3:4);

filen1='050901'
yy1=filen1(1:2);
mm1=filen1(3:4);

filen2='040901'
yy2=filen2(1:2);
mm2=filen2(3:4);

altitudeinterval= [9 11]; %km
ext='L'
tag='rand'
analyseflag=1


wl='WV'; %IR or WV
calib=[0.1 5; 0.01 6] %calibration constants, IR; WV
set(0,'defaultfigureposition',[220    298    560    420])
switch wl
   case 'IR'
      calibi=1
   case 'WV'
      calibi=2
end

dt=900;              %15 min
binsize=7200;        %120 min, time between points in figures

load(['xyzt00',yy,mm])
x1=x00;
T001=t000;

load(['xyzt00',yy1,mm1])
x2=x00;
T002=t000;

load(['xyzt00',yy2,mm2])
x3=x00;
T003=t000;

x=[x1;x2;x3];
t000=[T001;T002;T003];
load tt

jord=uint8(zeros(600,500));
   [longi latti]=ndgrid(1:600,1:500);
   [latt long]=refgeo(latti+2000 ,longi+800);
   mask=(latt>boxen(2)).*(latt<boxen(5)).*(long>boxen(1)).*(long<boxen(4));
%satellite pictures inside the box


D=dir(['eumetsat',yy,mm,'/OpenMTP_20',yy,'-',mm,'-*_*_712345_1_1_1.',wl])  %satellite
data
D1=dir(['eumetsat',yy1,mm1,'/OpenMTP_20',yy1,'-',mm1,'-*_*_712345_1_1_1.',wl])
D2=dir(['eumetsat',yy2,mm2,'/OpenMTP_20',yy2,'-',mm2,'-*_*_712345_1_1_1.',wl])

load(['rS',wl,filen])
rS1=rS(1:2,:,:);
s001=s00;

load(['rS',wl,filen1])
rS2=rS(1:2,:,:);
s002=s00;

load(['rS',wl,filen2])
rS3=rS(1:2,:,:);
s003=s00;

s00=[s001;s002;s003];
rS=rS1;
```

```
rS(:,749:(748+1251),:)= rS2;
rS(:,(748+1251+1):(748+1251+1150),:)=rS3;
clear rS1 rS2 rS3

S=squeeze(rS(1,:,1:2:end-1));
X=squeeze(x(:,1:2:end));
s01=zeros(size(S));
s02=squeeze(rS(2,:,1:2:end-1));

t1=tt(1:2:end-1);
t01=t000(:,1:2:end);
ttt=ones(size(t01,1),1)*t1;

Iout=find(mod(t1,24)<=1)
S(:,Iout)=0;
s01=s00(:,1:2:end);
I=((s01>0).*(S>0));
S=S.*I;
s01=s01.*I;
s02=s02.*I;
ttt=ttt.*I;

mdS=sum(S-s01)./sum(I);

Is=find(S>0);
 Isa=S>0;
 Ic=X>0;
 dIc=[(diff(Ic')'==-1),zeros(size(X,1),1)];
 Idx=((S>0).*(dIc>0));
 Idxa=((S>0).*(dIc>0));
 M=(sum(S.*Idxa)./sum(Idxa) - sum(S.*Isa)./sum(Isa));
 m= mean(M(find(isfinite(M))));

dS=S-s01;
dS2=S-s02;

IH=ceil((ttt-t01)*3600/binsize)+1;
H=zeros(size(dS,2),1);
Hs2=zeros(size(dS2,2),1);

H2=zeros(size(dS,2),1);
NH=zeros(size(dS,2),1);
for i=1:size(dS,1);
    for j=1:size(dS,2);
        if IH(i,j)>1
            H(IH(i,j))=H(IH(i,j))+dS(i,j);
            Hs2(IH(i,j))=Hs2(IH(i,j))+dS2(i,j);
            H2(IH(i,j))=H2(IH(i,j))+dS(i,j)^2;
            NH(IH(i,j))=NH(IH(i,j))+1;
        end
    end;
end;
%figure(3);

clf
plot(((1:size(H,1))-1).*binsize/3600,H./NH,'linew',2);
hold on
plot(((1:size(Hs2,1))-1).*binsize/3600,Hs2./NH,'r','linew',2);
sqrt((H2./NH-(H./NH).^2)/(90))
eb0=errorbar(((1:10:size(H,1))-
1).*binsize/3600,H(1:10:end)./NH(1:10:end),sqrt(H2(1:10:end)./(NH(1:10:end)-
(H(1:10:end)./NH(1:10:end)).^2)/90),'.','linew',2);
eb1=errorbar(((1:10:size(H,1))-1).*binsize/3600,Hs2(1:10:end)./NH(1:10:end),sqrt(
H2(1:10:end)./(NH(1:10:end)-(H(1:10:end)./NH(1:10:end)).^2)/90),'.r','linew',2);
xlim([0 100]);
errorbar_tick(eb0);
errorbar_tick(eb1);
title('Relative radiance WV: Three months','fontsize', 14)

ol=legend('Radiance relative to radiance at t0', 'Radiance relative to radiance in
(x0,y0)');
xlabel('Time /h','fontsize', 14),ylabel('W m^{-2}sr^{-1}','fontsize', 14);
joeexp(['fig/relrad_',wl,tag,'collect','_',num2str(altitudeinterval(1)),'_',num2str(al
titudeinterval(2))])
```